Analyzing the Optimality Gap between Linear and Nonlinear Multi-Period Optimal Power Flow Models of Active Distribution Networks

Aryan Ritwajeet Jha∗, *SIEEE*, Subho Paul†, *MIEEE*, and Anamika Dubey∗, *SMIEEE*
∗*School of Electrical Engineering & Computer Science*, *Washington State University*, Pullman, WA, USA
†*Department of Electrical Engineering*, *Indian Institute of Technology (BHU) Varanasi*, Varanasi, UP, India
∗{aryan.jha, anamika.dubey}@wsu.edu, †{subho.eee}@itbhu.ac.in

***Abstract*—Multi-period optimal power flow (MPOPF) frameworks are increasingly gaining attention due to the growing integration of battery-based distributed energy resources (DERs) in electricity distribution networks (EDNs). While MPOPF problems are typically formulated as non-convex programming (NCP) using non-convex branch power flow models, slow convergence and high computational requirements have spurred research into linear programming (LP)-based OPF approaches, which introduce an optimality gap. However, to the best of the authors' knowledge no current work has explicitly investigated how EDN size and DER penetration levels influence this gap. In this article, we develop multi-period OPF models for EDNs, comparing NCP- and LP-based solutions for networks of different scales—specifically, a 10-bus (small) and an IEEE-123-bus (medium) system—under varying DER deployments. We analyze the resulting optimality gap and degree of infeasiblity via OpenDSS simulations. Our findings indicate that while the optimality gap of LP-based methods grows with network size, these approaches still deliver near-optimal solutions and offer substantially faster convergence than their NCP counterparts.**

***Index Terms*—Battery energy storage systems, distribution system, optimal power flow, distributed energy resources.**

I. Introduction

Optimal power flow (OPF) techniques are utilized to efficiently manage controllable grid-edge resources to achieve various system-wide goals, including cost-effectiveness, reliability, and resilience [1]. OPF analysis is becoming increasingly important at the distribution level due to the rising integration of distributed energy resources (DERs), particularly photovoltaic (PV) systems and battery energy storage systems (BESS). BESS plays a crucial role in mitigating DER variability through controlled charging and discharging, ensuring a stable supply-demand balance [2]. However, incorporating BESS into OPF significantly increases the complexity of distribution network (DN) optimization, shifting the problem from a single-period, time-independent framework to a multi-period, time-coupled approach [3].

Conventional OPF methods rely on a central controller that collects grid-edge data, runs the OPF algorithm, and dispatches control signals to manage system resources. Therefore, those are named as centralized OPF (COPF), which are typically formulated as mixed-integer non-convex programming (MINCP) problems. A non-convex active-reactive OPF is formulated in [4] for scheduling the operation of BESS in DN. Safdarian et al. [5] investigated the impact of demand response programs on residential customers by directly solving the the MINCP based OPF problem. Mohapatra et al. [6] combined the gradient method and metaheuristic optimization for solving the MINCP framework. Padilha-Feltrin et al. [7] and Liu et al. [8] employed nondominated sorting genetic algorithm (NSGA-II) and improved grey wolf equilibrium optimizer for solving the MINCP based OPF problems, respectively. Previously, authors also solved the MINCP based OPF for determining the operation of batteries in DN [9].

For making the MINCP OPF models convex, Li et al. [10] proposed a linear power flow model by merging support vector regression (SVR) and ridge regression (RR) algorithms. Lei et al. [11] proposed a privacy-preserving linear OPF model for multi-agent DN having privately owned grid resources. Linear approximation of the non-convex power flow model with Taylor series expansion for reactive power optimization is suggested in [12] and [13]. Vaishya et al. [14] designed a linear ACOPF model for DN using active and reactive power sensitivity factors.

Following research gaps are identified from the above literature survey:

1) Direct solution of MINCP framework, [4], [5], [9] may provide the global optimal solution but the solution time is more and mostly efficient for small and medium-sized DNs. They possess slow convergence and sometimes fail to converge for bulk DNs.
2) Metaheuristic optimizations, [6]–[8], may stuck at the local optimum solution and suffer from slow convergence for multi-variate problems.
3) Linear programming frameworks, [10]–[14], are fast converging. However, they possess an optimality gap in the derived solutions and the impact of the size of the network on the optimality gap is not investigated in the existing research works.

To overcome the above mentioned research gaps, this article aims to investigate the impact of the size of the network on the value of the optimality gap between the solutions obtained from non-linear and linear multi-period OPF models for DNs. The overall study has the following distinguished features:

1) At first, the multi-period OPF problem is formulated for

DNs consisting of battery-associated solar power generation as both non-linear and linear optimization problems. The non-linear problem is formulated by considering the original non-convex branch flow model of DNs [15]. In contrast, the linear framework is developed by considering the LinDistFlow model of DN [16]. Further, the quadratic inequality constraints are linearized by employing the hexagonal approximation technique.

2) The investigation is carried out for distribution networks with different sizes like small (10-bus), medium (IEEE 123-bus), and large (730-bus) with different penetration levels of DERs and batteries.
3) The ACOPF feasibility of the derived solutions is validated by feeding the determined control outputs in OpenDSS platform.

II. Problem Formulation

A. Notations

In this study, the distribution system is modeled as a tree (connected graph) with N number of buses (indexed with i, j, and k); the study is conducted for T time steps (indexed by t), each of interval length Δt. The sets of buses with DERs and batteries are D and B respectively, such that $D, B \subseteq N$. A directed edge from bus i to j in the tree is represented by ij and the set for edges is given by $\mathcal{L}$. Line resistance and reactance are r_{ij} and x_{ij}, respectively. Magnitude of the current flowing through the line at time t is denoted by I_{ij}^t and $l_{ij}^t = \left(I_{ij}^t\right)^2$. The voltage magnitude of bus j at time t is given by V_j^t and $v_j^t = \left(V_j^t\right)^2$. Apparent power demand at a node j at time t is $s_{L_j}^t$ $(= p_{L_j}^t + jq_{L_j}^t)$. The active power generation from the DER present at bus j at time t is denoted by $p_{D_j}^t$ and controlled reactive power dispatch from the DER inverter is $q_{D_j}^t$. DER inverter capacity is $S_{D_{R_j}}$. The apparent power flow through line ij at time t is S_{ij}^t $(= P_{ij}^t + jQ_{ij}^t)$. The real power flowing from the substation into the network is denoted by P_{Subs}^t and the associated cost involved per kWh is C^t. The battery energy level is B_j^t. Charging and discharging active power from battery inverter (of apparent power capacity $S_{B_{R_j}}$) are denoted by $P_{c_j}^t$ and $P_{d_j}^t$, respectively and their associated efficiencies are η_c and η_d, respectively. The energy capacity of the batteries is denoted by B_{R_j}, and the rated battery power is $P_{B_{R_j}}$. soc_{min} and soc_{max} are fractional values for denoting safe soc limits of a battery about its rated state-of-charge (soc) capacity. The reactive power support of the battery inverter is indicated by $q_{B_j}^t$.

B. MPOPF Model Descriptions

In this section, a head to head comparison of the constraints used for both the nonlinear and linear models is provided for the Multi-Period Optimal Power Flow (MPOPF) problem. For the nonlinear formulation, the branch flow model (BFM-NL) [15] is used, while for the linear formulation, the LinDistFlow variation of the Branch Flow Model [17] is used. It may be seen that barring a few constraints, most of the constraints are common between the two models as described by (1) to (16). The uncommon constraints are suffixed with an '-NL' for the nonlinear model and an '-L' for the linear model.

(1) describes the objective function of the MPOPF problem. Specifically, for the problem of minimizing the cost of the power borrowed from the substation f_0. The inclusion of a secondary 'Battery Loss' function f_{SCD} penalizes the simultaneous charging and discharging of batteries, while avoiding the need of binary variables [18].

$$\min \sum_{t=1}^{T} \left\{ f_0^t + f_{SCD}^t \right\} \tag{1}$$

where

$$f_0^t = C^t P_{Subs}^t \Delta t$$

$$f_{SCD}^t = \alpha \sum_{j \in \mathcal{B}} \left\{ (1 - \eta_C) P_{C_j}^t + \left(\frac{1}{\eta_D} - 1 \right) P_{D_j}^t \right\}$$

Subject to the constraints (2NL) to (16) as given below:

$$\sum_{(j,k)\in\mathcal{L}} \left\{ P_{jk}^t \right\} - \left(P_{ij}^t - r_{ij} l_{ij}^t \right) = p_j^t \tag{2NL}$$

$$\sum_{(j,k)\in\mathcal{L}} \left\{ P_{jk}^t \right\} - \left(P_{ij}^t \right) = p_j^t \tag{2L}$$

$$p_j^t = \left(P_{d_j}^t - P_{c_j}^t \right) + p_{D_j}^t - p_{L_j}^t \tag{3}$$

$$\sum_{(j,k)\in\mathcal{L}} \left\{ Q_{jk}^t \right\} - \left(Q_{ij}^t - x_{ij} l_{ij}^t \right) = q_j^t \tag{4NL}$$

$$\sum_{(j,k)\in\mathcal{L}} \left\{ Q_{jk}^t \right\} - \left(Q_{ij}^t \right) = q_j^t \tag{4L}$$

$$q_j^t = q_{D_j}^t + q_{B_j}^t - q_{L_j}^t \tag{5}$$

$$v_j^t = v_i^t - 2(r_{ij} P_{ij}^t + x_{ij} Q_{ij}^t) + \left\{ r_{ij}^2 + x_{ij}^2 \right\} l_{ij}^t \tag{6NL}$$

$$v_j^t = v_i^t - 2(r_{ij} P_{ij}^t + x_{ij} Q_{ij}^t) \tag{6L}$$

$$(P_{ij}^t)^2 + (Q_{ij}^t)^2 = l_{ij}^t v_i^t \tag{7NL}$$

$$P_{Subs}^t \geq 0 \tag{8}$$

$$v_j^t \in \left[V_{min}^2, V_{max}^2 \right] \tag{9}$$

$$q_{D_j}^t \in \left[-q_{D_{Max,j}}^t, q_{D_{Max,j}}^t \right] \tag{10}$$

$$q_{D_{Max,j}}^t = \sqrt{{S_{D_{R,j}}}^2 - {p_{D_j}^t}^2} \tag{11}$$

$$B_j^t = B_j^{t-1} + \Delta t \left(\eta_c P_{c_j}^t - \frac{1}{\eta_d} P_{d_j}^t \right) \tag{12}$$

$$P_{c_j}^t, P_{d_j}^t \in \left[0, P_{B_{R,j}} \right] \tag{13}$$

$$(P_{B_j}^t)^2 + (q_{B_j}^t)^2 \leq S_{B_{R,j}}^2 \tag{14NL}$$

TABLE I: Parameter values

Parameter	Value
V_{min}, V_{max}	0.95 pu, 1.05 pu
$p_{D_{R,j}}$	$0.33p_{L_{R,j}}$
$S_{D_{R,j}}$	$1.2p_{D_{R,j}}$
$P_{B_{R,j}}$	$0.33p_{L_{R,j}}$
$S_{B_{R,j}}$	$1.2P_{B_{R,j}}$
$B_{R,j}$	$T_{fullCharge} \times P_{B_{R,j}}$
$T_{fullCharge}$	4 h
Δt	1 h
η_c, η_d	0.95, 0.95
soc_{min}, soc_{max}	0.30, 0.95
α	0.001

$$q^t_{B_j} \in \left[-\sqrt{3}(P^t_{B_j} + S_{B_{R,j}}), -\sqrt{3}(P^t_{B_j} - S_{B_{R,j}})\right] \quad \text{(14L-a)}$$

$$q^t_{B_j} \in \left[-\frac{\sqrt{3}}{2}S_{B_{R,j}}, \frac{\sqrt{3}}{2}S_{B_{R,j}}\right] \quad \text{(14L-b)}$$

$$q^t_{B_j} \in \left[\sqrt{3}(P^t_{B_j} - S_{B_{R,j}}), \sqrt{3}(P^t_{B_j} + S_{B_{R,j}})\right] \quad \text{(14L-c)}$$

$$P^t_{B_j} = P^t_{d_j} - P^t_{c_j} \quad (15)$$

$$B^t_j \in [soc_{min}B_{R,j}, soc_{max}B_{R,j}] \quad (16)$$

The network power flow constraints, notably, the nodal real and reactive power balance equations and the KVL constraint across a branch, are similar across the two models, with the only difference being whether a term representing losses is included (2NL, 4NL,6NL) or not (2L,4L,6L) not.

Backflow of real power into the substation from the distribution system is avoided using the constraint (8). The allowable limits for bus voltages are modeled via (9). (10) and (11) describe the reactive power limits of DER inverters. The trajectory of the battery energy versus time is given by (12) (this is a time-coupled constraint). Battery charging and discharging powers are limited by the battery's rated power capacity, as given by (13). Reactive Power Output from Battery Inverters are is constrained by the quadratic inequality (14NL). A linearized set of equations approximating the same are given by (14)L, which utilize a hexagonal approximation of the inequality [19]. For the safe and sustainable operation of the batteries, the energy B^t_j is constrained to be within some percentage limits of the rated battery SOC capacity, modeled using (16)

C. Linear MPOPF with Batteries

III. Case Study Demonstration

IV. Conclusions

References

[1] A. Dubey and S. Paudyal, "Distribution system optimization to manage distributed energy resources (ders) for grid services," Foundations and Trends® in Electric Energy Systems, vol. 6, no. 3-4, pp. 120–264, 2023. [Online]. Available: http://dx.doi.org/10.1561/3100000030

[2] T. Gangwar, N. P. Padhy, and P. Jena, "Storage allocation in active distribution networks considering life cycle and uncertainty," IEEE Trans. Ind. Inform., vol. 19, no. 1, pp. 339–350, Jan. 2023.

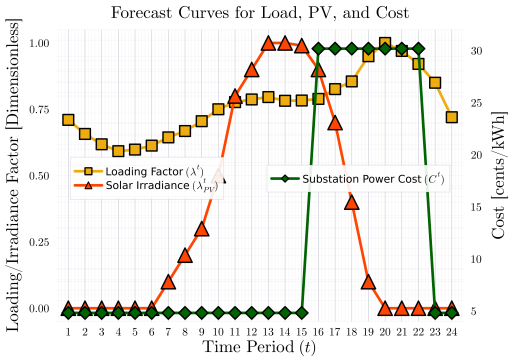

Fig. 1: Forecasts for demand power, irradiance and cost of substation power over a 24 hour horizon

TABLE II: MPOPF performance comparison - ADS10 test system for 24h

Metric	BFM-NL	LinDistFlow
Full horizon		
Substation power cost ($)	204.27	204.28
Substation real power (kW)	1528.35	1528.4
Line loss (kW)	0.28	0.33
Substation reactive power (kVAR)	428.9	795.56
PV reactive power (kVAR)	174.41	-0.69
Battery reactive power (kVAR)	192.8	-0.37
Computation		
Total Simulation Time (s)	2.64	0.77

[3] S. Paul and N. P. Padhy, "A new real time energy efficient management of radial unbalance distribution networks through integration of load shedding and cvr," IEEE Trans. Power Del., vol. 37, no. 4, pp. 2571–2586, 2022.

[4] A. Gabash and P. Li, "Active-reactive optimal power flow in distribution networks with embedded generation and battery storage," IEEE Trans. Power Syst., vol. 27, no. 4, pp. 2026–2035, 2012.

[5] A. Safdarian, M. Fotuhi-Firuzabad, and M. Lehtonen, "Benefits of demand response on operation of distribution networks: A case study," IEEE Syst. J., vol. 10, no. 1, pp. 189–197, 2016.

[6] A. Mohapatra, P. R. Bijwe, and B. K. Panigrahi, "An efficient hybrid approach for volt/var control in distribution systems," IEEE Trans. Power Del., vol. 29, no. 4, pp. 1780–1788, 2014.

[7] A. Padilha-Feltrin, D. A. Quijano Rodezno, and J. R. S. Mantovani, "Volt-var multiobjective optimization to peak-load relief and energy efficiency in distribution networks," IEEE Trans. Power Del., vol. 30, no. 2, pp. 618–626, 2015.

[8] W. Liu, Z. Ding, H. Zhang, and M. Zhu, "Multiobjective optimal power flow for distribution networks utilizing a novel heuristic algorithm—grey wolf equilibrium optimizer," IEEE Syst. J., vol. 18, no. 1, pp. 174–185, 2024.

[9] A. R. Jha, S. Paul, and A. Dubey, "Spatially distributed multi-period optimal power flow with battery energy storage systems," in 2024 56th North American Power Symposium (NAPS), 2024, pp. 1–6.

[10] P. Li, W. Wu, X. Wang, and B. Xu, "A data-driven linear optimal power flow model for distribution networks," IEEE Trans. Power Syst., vol. 38, no. 1, pp. 956–959, 2023.

[11] C. Lei, S. Bu, Q. Chen, Q. Wang, Q. Wang, and D. Srinivasan, "Decentralized optimal power flow for multi-agent active distribution networks: A differentially private consensus admm algorithm," IEEE Trans. Smart Grid, vol. 15, no. 6, pp. 6175–6178, 2024.

[12] S. Paul and N. P. Padhy, "Real-time advanced energy-efficient management of an active radial distribution network," IEEE Syst. J., vol. 16, no. 3, pp. 3602–3612, Sept. 2022.

[13] T. Yang, Y. Guo, L. Deng, H. Sun, and W. Wu, "A linear branch flow model for radial distribution networks and its application to reactive power optimization and network reconfiguration," IEEE Trans. Smart Grid, vol. 12, no. 3, pp. 2027–2036, 2021.

[14] S. R. Vaishya, A. R. Abhyankar, and P. Kumar, "A novel loss sensitivity

TABLE III: MPOPF feasibility comparison - ADS10 test system for 24h

Metric	BFM-NL	LinDistFlow
Max. all-time discrepancy		
Voltage (pu)	0.00001	0.00001
Line loss (kW)	0.000009	0.000006
Substation power (kW)	0.000014	0.02410
Substation reactive power (kVAR)	0.070706	0.05618

TABLE IV: MPOPF performance comparison - IEEE123-A test system for 24h

Metric	BFM-NL	LinDistFlow$^{\mathbb{D}}$
Largest subproblem		
Decision variables	15144	12096
Linear constraints	18456	22200
Nonlinear constraints	3672	0
Simulation results		
Substation power cost ($)	2787.44	2798.4
Substation real power (kW)	20984.89	21065.89
Line loss (kW)	380.09	461.38
Substation reactive power (kVAR)	6835.82	12259.29
PV reactive power (kVAR)	1972.27	195.12
Battery reactive power (kVAR)	3709.71	204.63
Computation		
Total Simulation Time (s)	17.44	0.85

based linearized opf and lmp calculations for active balanced distribution networks," IEEE Syst. J., vol. 17, no. 1, pp. 1340–1351, 2023.

[15] M. Farivar and S. H. Low, "Branch flow model: Relaxations and convexification—part i," IEEE Transactions on Power Systems, vol. 28, no. 3, pp. 2554–2564, 2013.

[16] L. Gan and S. H. Low, "Convex relaxations and linear approximation for optimal power flow in multiphase radial networks," in 2014 Power Systems Computation Conference. Poland: IEEE, pp. 18–22.

[17] M. Farivar, L. Chen, and S. Low, "Equilibrium and dynamics of local voltage control in distribution systems," in 52nd IEEE Conference on Decision and Control. IEEE, pp. 10–13.

[18] N. Nazir and M. Almassalkhi, "Guaranteeing a Physically Realizable Battery Dispatch Without Charge-Discharge Complementarity Constraints," IEEE Trans. Smart Grid, vol. 14, no. 3, pp. 2473–2476, Sep. 2021.

[19] H. Ahmadi and J. R. Martı', "Linear Current Flow Equations With Application to Distribution Systems Reconfiguration," IEEE Trans. Power Syst., vol. 30, no. 4, pp. 2073–2080, Oct. 2014.

TABLE V: MPOPF feasibility comparison - IEEE123-A tests system for 24h

Metric	BFM-NL	LinDistFlow
Max. all-time discrepancy		
Voltage (pu)	0.00007	0.00206
Line loss (kW)	0.01818	1.8074
Substation power (kW)	0.43164	32.362
Substation reactive power (kVAR)	1.0102	64.403

TABLE VI: MPOPF performance comparison - IEEE123-B test system for 24h

Metric	BFM-NL	LinDistFlow$^{\mathbb{D}}$
Largest subproblem		
Decision variables	17184	14136
Linear constraints	24168	30360
Nonlinear constraints	4080	0
Simulation results		
Substation power cost ($)	1973.83	1987.78
Substation real power (kW)	16594.11	16693.01
Line loss (kW)	234.78	333.78
Substation reactive power (kVAR)	-404.91	11055.41
PV reactive power (kVAR)	7255.22	1535.29
Battery reactive power (kVAR)	5371.97	-190.93
Computation		
Total Simulation Time (s)	23.75	1.66

TABLE VII: MPOPF feasibility comparison - IEEE123-B test system for 24h

Metric	BFM-NL	LinDistFlow
Max. all-time discrepancy		
Voltage (pu)	0.000059	0.001599
Line loss (kW)	0.00776	1.055093
Substation power (kW)	0.217433	23.344019
Substation reactive power (kVAR)	1.016894	45.925288

TABLE VIII: MPOPF performance comparison - IEEE730 test system for 24h

Metric	BFM-NL	LinDistFlow$^{\mathbb{D}}$
Largest subproblem		
Decision variables	00000	67224
Linear constraints	00000	131616
Nonlinear constraints	0000	0
Simulation results		
Substation power cost ($)	0000	1539.4
Substation real power (kW)	0000	12313.19
Line loss (kW)	0000	176.41
Substation reactive power (kVAR)	0000	4626.23
PV reactive power (kVAR)	0000	-18.69
Battery reactive power (kVAR)	0000	-14.33
Computation		
Total Simulation Time (s)	0000	7.67

TABLE IX: MPOPF feasibility comparison - IEEE730 test system for 24h

Metric	BFM-NL	LinDistFlow
Max. all-time discrepancy		
Voltage (pu)	0000	0.0227
Line loss (kW)	0000	2.6696
Substation power (kW)	0000	12.1844
Substation reactive power (kVAR)	0000	7.3131